Journal of Marine Research, 77, 297–324, 2019

The regulation of oxygen to low concentrations in marine oxygen-minimum zones

by Don E. Canfield[1,2,3], Beate Kraft[1], Carolin R. Löscher[1], Richard A. Boyle[1], Bo Thamdrup[1], and Frank J. Stewart[4]

ABSTRACT

The Bay of Bengal hosts persistent, measurable, but sub-micromolar, concentrations of oxygen in its oxygen-minimum zone (OMZ). Such low-oxygen conditions are not necessarily rare in the global ocean and seem also to characterize the OMZ of the Pescadero Basin in the Gulf of California, as well as the outer edges of otherwise anoxic OMZs, such as can be found, for example, in the Eastern Tropical North Pacific. We show here that biological controls on oxygen consumption are required to allow the semistable persistence of low-oxygen conditions in OMZ settings; otherwise, only small changes in physical mixing or rates of primary production would drive the OMZ between anoxic and oxic states with potentially large swings in oxygen concentration. We propose that two controls are active: an oxygen-dependent control on oxygen respiration and an oxygen inhibition of denitrification. These controls, working alone and together, can generate low-oxygen concentrations over a wide variability in ocean mixing parameters. More broadly, we discuss the oxygen regulation of organic matter cycling and N_2 production in OMZ settings. Modern biogeochemical models of nitrogen and oxygen cycling in OMZ settings do contain some of the parameterizations that we explore here. However, these models have not been applied to understanding the persistence of low, but measurable, concentrations of oxygen in settings like the Bay of Bengal, nor have they been applied to understanding what biological/physical processes control the transition from a weakly oxygenated state to a "functionally" anoxic state with implications for nitrogen cycling. Therefore, we believe that the approach here illuminates the relationship between oxygen and the biogeochemical cycling of carbon and nitrogen in settings like the Bay of Bengal. Furthermore, we believe that our results could further inform large-scale ocean models seeking to explore how global warming might influence the spread of low-oxygen waters, influencing the cycles of oxygen, carbon, and nitrogen in OMZ settings.

Keywords: oxygen-minimum zone, OMZ, denitrification, aerobic respiration, climate change, model, feedback, Bay of Bengal

1. NordCEE and Department of Biology, University of Southern Denmark, Campusvej 55, 5230 Odense M, Denmark.
2. Corresponding author: ***e-mail: dec@biology.sdu.dk***
3. Villum Investigator, Villum Foundation, Tobaksvejen 10, 2860 Søborg, Denmark.
4. School of Biology, Georgia Institute of Technology, Atlanta GA 30332-0230.

1. Introduction

Generally speaking, oxygen-minimum zones (OMZs) are distributed throughout the global ocean, in which, typically, surface waters and deep waters are oxygen-enriched compared to waters at intermediate depths (Broecker and Peng 1982). Surface waters remain well-oxygenated owing to equilibrium exchange with the atmosphere, whereas deep waters inherit their high oxygen concentrations from the high-latitude surface waters in which they originate (Broecker and Peng 1982; Broecker 1974). Waters of intermediate water depth become reduced in oxygen concentration as settling organics from the photic zone decompose. In some regions of the global ocean, in particular the North and South Tropical Eastern Pacific and in the Arabian Sea, oxygen concentrations become reduced to lower than measurable with the most sensitive available methods (Jensen et al. 2011; Revsbech et al. 2009; Thamdrup et al. 2012; Tiano et al. 2014). These waters accumulate nitrite, which is otherwise unstable in the presence of oxygen (Thamdrup et al. 2012), and support an active nitrogen cycle including the processes of denitrification and anammox (Cline and Kaplan 1975; Codispoti and Packard 1980; Jensen et al. 2011; Lam et al. 2009; Morrison et al. 1999; Naqvi 1991; Thamdrup et al. 2012). Such environments are referred to as oxygen-depleted zones (ODZs).

Other environments, such as the Bay of Bengal, for example, display exceptionally low, but still measurable (with new high-sensitivity oxygen sensors; Revsbech et al. 2009), oxygen concentrations in the 5 to 500 nM range. These low-oxygen levels are sufficient to support the efficient biological oxidation of nitrite to nitrate (Bristow et al. 2017). Slightly oxygenated conditions are apparently a common, if not persistent, feature of the Bay of Bengal water column as previous studies have indicated oxygen levels below detection with the less sensitive methods, but also with no nitrite accumulation (Naqvi et al. 2005), indicating some oxygen availability (Thamdrup et al. 2012). A similar situation apparently exists in the Pescadero Basin of the Gulf of California, in which oxygen concentrations are below detection with traditional methods, but nitrite does not accumulate (Rago et al. 2013). There is also a zone with undetectable oxygen [with CTD (conductivity, temperature, depth)] and no nitrite accumulation in the upper 120 meters of ODZ in southern Eastern Tropical North Pacific (ETNP; Chronopoulou et al. 2017), and one might expect a similar situation at the outer edges of otherwise anoxic ODZs. For example, in the outer reaches of the ETNP ODZ, oxygen concentrations fluctuate between 0 and 2 μM over hundreds of meters of water depth (Fig. 1), whereas oxygen is undetectable further towards shore (Fig. 1). Therefore, low-oxygen conditions, such as those found in the Bay of Bengal, may not be uncommon. We emphasize that these low oxygen concentrations are measurable and greater than those found in the core of "traditional" ODZs as discussed above.

What, then, are the oxygen concentrations in "traditional" ODZs where nitrite accumulates? Indeed, we cannot currently measure oxygen concentrations to such low levels, but we believe that they are extremely low: probably sub-nM and possibly in the low pM range or even lower. Thus, experiments on the low-oxygen metabolism of *Escherichia coli*

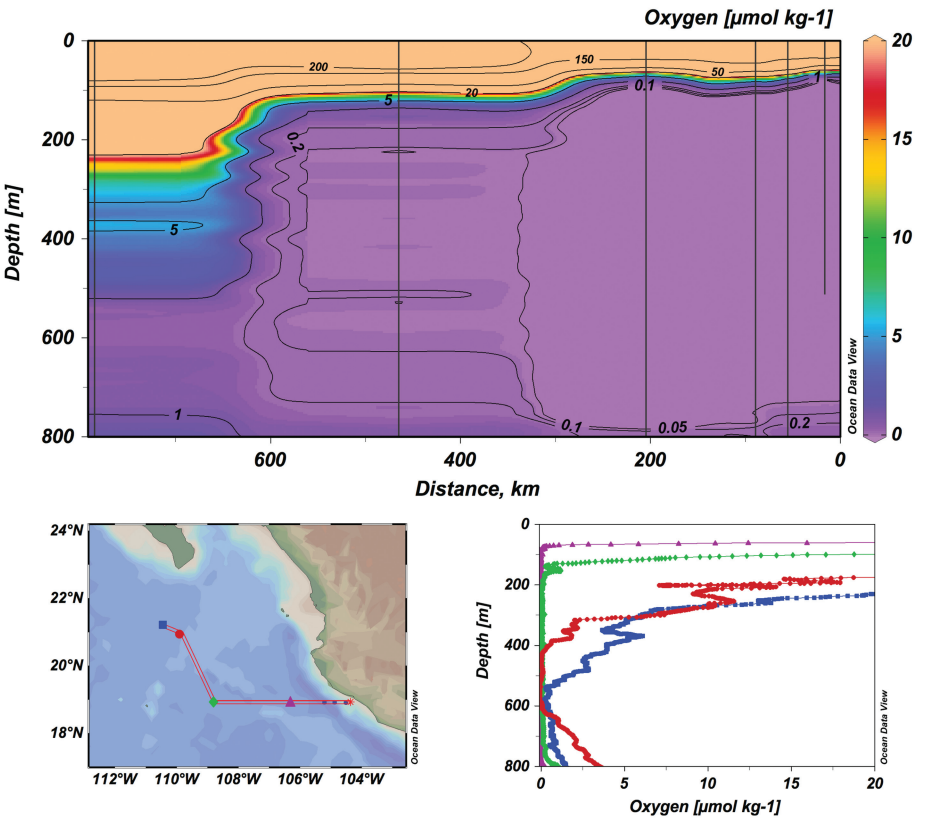

Figure 1. Oxygen distribution for sites from the outer edges of the oxygen-minimum zone (OMZ) in the Eastern Tropical North Pacific (ETNP). Sampling sites indicated by vertical lines in the upper figure. Also, in the upper figure, onshore-offshore moves from left to right. The oxygen profile from the 3 inner sites is indistinguishable from the purple data in the triangles on graph on lower right.

suggest that this organism can probably metabolize oxygen and grow in the sub-nM range (Stolper et al. 2010). Furthermore, the kinetics of nitrite oxidation by oxygen with natural populations of nitrifiers is best explained if oxygen is utilized with 2 apparent k_m values: one with a relatively high value of 1750 $\pm$ 570 nM and another with an extremely low, sub-nM k_m of 0.5 $\pm$ 4 nM (Bristow et al. 2016). Such a low k_m value for nitrification would drive oxygen into the lower pM range as nitrite accumulates. Although we cannot yet place a lower limit on oxygen concentrations in ODZs, in what follows, we will refer to waters in nitrite-accumulating ODZs as functionally anoxic.

Returning to the Bay of Bengal, the long-term maintenance of measurable, but low, oxygen concentrations is a challenge to understand. Thus, in simple box models of oxygen-minimum zone biogeochemistry, low-oxygen conditions are transient and inherently

unstable (Canfield 2006). For example, without any controls on oxygen utilization, only small changes in upwelling rate or mixing rate can drive OMZ waters between an oxygenated and an anoxic state (Canfield 2006). The maintenance of sub-μM levels of oxygen would require exquisite long-term consistency in physical mixing rates and rates of primary production. Such consistency, however, is difficult to imagine in any marine environment.

This means that oxygen-dependent biological controls on oxygen utilization are likely involved in establishing a semistable state of persistently measurable, but low, oxygen concentrations in marine OMZs where such situations are found. In what follows, we will refer to these controls as feedbacks, and we can identify two such biological feedbacks that may be active. One is oxygen respiration. Oxygen-respiring heterotrophs in OMZ settings have oxidase enzymes whose affinities for oxygen can vary by two orders of magnitude (Kalvelage et al. 2015), and rates of oxygen respiration have been shown to depend on oxygen concentration in low-oxygen waters from natural settings (Devol 1978; Garcia-Robledo et al. 2016; Kalvelage et al. 2015), as well as in pure bacterial cultures (Gong et al. 2016; Stolper et al. 2010). A negative feedback on oxygen utilization would occur if oxygen respiration rate slowed at lower oxygen concentrations, helping to maintain low-oxygen concentrations in OMZ waters. Another feedback is related to denitrification. In OMZ environments, some denitrification can occur in the presence of oxygen, but denitrification rates typically become progressively more inhibited as oxygen concentrations increase (Babbin et al. 2014; Dalsgaard et al. 2014). Denitrification removes a key nutrient, nitrogen, from the biologically available nitrogen pool. Therefore, enhanced denitrification at low-oxygen levels, by removing nitrogen, could provide a negative feedback on primary production and thus limit the carbon available for oxic respiration in low-oxygen waters. This could also serve to maintain low-oxygen levels. We will also discuss the possible role of anammox as a negative feedback on the regulation of oxygen concentration in OMZ settings.

We note that another physiological feedback has been proposed to limit full deoxygenation in OMZ settings (Zakem and Follows 2017). This feedback is based on the physiological limitations of aerobes at low-oxygen levels combined with consideration of their life cycles. The basic idea is that, depending on the size of the organism, the metabolism and growth rate of an aerobe becomes limited by the concentration of oxygen (see, also, Stolper et al. 2010). This is somewhat analogous to the oxygen limitation of aerobic respiration rates as explored above, but, in addition, there becomes a critical limiting oxygen concentration at which the growth rate of an aerobic population cannot keep pace with its rate of death or other loss terms. At this critical oxygen concentration, anaerobic carbon metabolisms ensue (like denitrification, for example) leaving residual unused oxygen. This is an intriguing idea, but it is seemingly based on the idea that facultative aerobes cannot simultaneously conduct aerobic and anaerobic metabolism. However, *Escherichia coli*, for example, switches gradually between aerobic and anaerobic metabolism as oxygen becomes limiting (Tseng et al. 1996). This is likely true for facultative aerobes in general, meaning that a facultative aerobe can stay viable even under extremely low oxygen concentrations, while still metabolizing oxygen, but growing predominantly from anaerobic metabolisms. Thus, as noted above,

our view is that ODZs accumulating nitrite maintain immeasurably low levels of oxygen, well below the critical levels envisioned by Zakem and Follows (2017), and at levels that we call functionally anoxic. We do, however, incorporate the idea of Zakem and Follows (2017) in that oxygen concentrations influence metabolic rates and the switch to anaerobic metabolism. We also agree, as explored below, that the processes driving ODZs to functional anoxia, as well as what oxygen levels this implies, are a challenge to understand.

More advanced models of OMZ geochemistry incorporate some of the feedbacks explored here, including the oxygen inhibition of denitrification and the oxygen control on oxic respiration (e.g., Al Azhar et al. 2014; Gutknecht et al. 2013; Sankar et al. 2018; Penn et al. 2016; Anderson 2007), and most of these models also include considerations of microbial growth, grazing, mortality, and biomass settling. The model of Penn et al. (2016) is noteworthy in concluding that microbial respiration kinetics control the spread of low-oxygen environments as ODZs expand due to global warming, a conclusion compatible with the model results presented here. However, as far as we are aware, advanced OMZ models have not yet addressed the problem of the persistence of low-oxygen conditions in OMZ environments. We believe that is best done by specifically exploring this problem with simple models (see Franks 2002). Therefore, we isolate this problem and explore the biological circumstances controlling the maintenance of low, but measurable, oxygen concentrations in OMZ environments and their potential spread through climate change (Keeling et al. 2010; Stramma et al. 2008). The implications of these biological controls and carbon and nitrogen cycling are also discussed.

2. Materials and Methods

Oxygen profiles were measured in the ETNP off Central Mexico during the OMZoMBiE (Oxygen Minimum Zone Microbial Biogeochemistry Expedition) cruise (R/V New Horizon, 13–28 June, 2013) using a Seabird 911plus CTD (Bellevue, Washington, USA) equipped with an SBE43 oxygen sensor. A zero correction was performed based on the oxygen reading at functionally anoxic depths as identified by parallel measurements with a STOX oxygen sensor (detection limit 9 nM; Ganesh et al. 2015; as previously described by Thamdrup et al. 2012).

3. The Model

We explore with a simple steady-state box model the factors that may regulate oxygen to low levels in OMZ-type settings. Used here is a 5-box model based on the model presented by Canfield (2006) and shown in Figure 2. The upper box (U) represents the surface ocean in the OMZ environment, and primary production occurs here as driven by the upwelling and mixing of nitrate into the box. Nitrate is assumed to be the limiting nutrient, and this model does not include nitrogen fixation. Indeed, low rates of nitrogen fixation are found in many OMZ environments when compared to rates of N_2 production by denitrification and anammox (Fernandez et al. 2011; Jayakumar et al. 2017), although in sulfidic ODZ

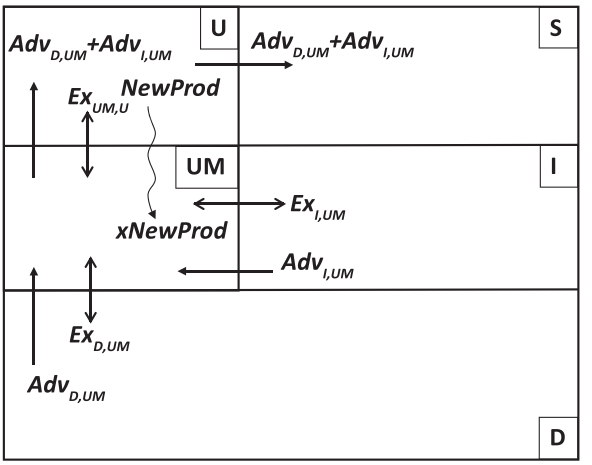

Figure 2. Five-box model used to explore the influence of oxygen control on aerobic respiration and denitrification in regulating oxygen to low concentration in oxygen-minimum zone (OMZ) waters. The model is based on that presented in Canfield (2006).

settings, nitrogen fixation is more important (Loescher et al. 2014). The *UM* box is where the oxygen-minimum develops as driven by the respiration of organic matter (*NewProd*) settling from the upper box. Depending on the modeling scenario, as developed below, this box may also include denitrification. The deep box (*D*) advects ($Adv_{D,UM}$) water into the *UM* box, where mixing also exchanges ($Ex_{D,UM}$) water between these boxes. The *UM* box has no specified dimension but is rather meant to represent a characteristic OMZ environment. For this reason, all the fluxes into and out of this box, and all of the other boxes, are presented per unit area (Table 1).

The *I* box represents water at intermediate depths and has chemical properties similar to those found at the outer reaches of OMZ environments, in which oxygen concentrations are reduced compared to the surface and deep water but elevated compared to those in the *UM* box. There is an advective flow ($Adv_{I,UM}$) of water from the intermediate box (*I*) into the *UM* box, as well as horizontal mixing exchange ($Ex_{I,UM}$) between the *I* box and the *UM* box. The value of the mixing parameter ($Ex_{I,UM}$) was determined on basis of the characteristic length in the ETSP between where the *UM* box expresses its characteristic chemistry and where the *I* box expresses its characteristic chemistry (Canfield 2006). The *S* box is not active and represents the surface ocean and the repository for the water advecting through the OMZ environment. This model is not a "closed model" in that water and chemistry enter and exchange (through the *I* and *D* boxes) and leave (through the *S* box) in reservoirs connected to the open ocean with characteristic chemistries for these large oceanic provinces. Thus, the model is a "flow-through" type model and does not consider global scale mass balance. However, water and mass are conserved within the boundaries of the model as expressed through the conservation equations as developed below.

Table 1. Parameters used in modelling (from Canfield 2006).

Parameter	Description	Value	Units
$Ex_{UM,U}$	Vertical exchange	0.03[a]	$cm^2\ s^{-1}$
$Ex_{D,UM}$	Vertical exchange	0.1	$cm^2\ s^{-1}$
$Ex_{I,UM}$	Horizontal exchange	0.4	$cm^2\ s^{-1}$
$Adv_{D,UM}$	Upwelling rate	0	$cm\ h^{-1}$
$Adv_{I,UM}$	Upwelling rate	Variable	$cm\ h^{-1}$
x	Fraction of *newprod* minerialized in *UM* box	0.7 (and variable)	Dimensionless
y	Proportion of *newprod* undergoing O_2 dependent respiration in *UM* box	Variable	Dimensionless
z	Proportion of O_2 dependent respiration channeled through denitrification	Variable	Dimensionless
O_U	Upper water O_2 concentration in upwelling zone	240	μM
O_D	Deep water O_2 concentration in upwelling zone	140	μM
O_I	Intermediate water O_2 concentration adjacent to *UM* box	40	μM
N_U	Surface water nitrate concentration	0	μM
N_D	Deep water nitrate concentration	36.65	μM
N_I	Intermediate water nitrate concentration	36	μM
r_a	O_2-used/NO_3-produced during OC oxidation	11	Dimensionless
r_n	Ratio between N liberated as N_2 during by denitrification compared to N liberated during oxic respiration	5.9	Dimensionless
k_m	Half-saturation constant for oxic respiration	400	nM
k_{mn}	Half-inhibition constant for denitrification	1,000	nM

Notes: [a]lower value used than in Canfield (2006) to mimic inhibition of vertical mixing in Bay of Bengal in surface waters owing to strong salinity stratification.

All mixing parameters (and other model parameters) used are summarized in Canfield (2006) and are reproduced in Table 1. These values are considered typical for OMZ environments. Four different modelling scenarios will be explored below: Model A, no feedbacks on oxygen respiration or denitrification; Model B, an oxygen control on oxygen respiration; Model C, an oxygen inhibition of denitrification; and Model D, both an oxygen control on

oxygen respiration and an oxygen inhibition of denitrification. Results will be discussed in light of measured or inferred rates of processes in Bay of Bengal waters and carbon flow through OMZ settings.

a. No feedbacks on oxygen respiration or denitrification

This is essentially the model presented in Canfield (2006). In developing this model, steady-state nitrate balances are written for the upper and lower boxes such that, for the upper box,

$$\begin{aligned} &N_{UM}\left(Adv_{D,UM} + Adv_{I,UM}\right) + Ex_{UM,U}(N_{UM} - N_U) \\ &\quad = N_U\left(Adv_{D,UM} + Adv_{I,UM}\right) + NewProd \end{aligned} \tag{1}$$

Where N_U represent the nitrate concentration in U box and N_{UM} the nitrate concentration in the UM box. With N_U assumed to be zero, equation 1 reduces to

$$N_{UM}\left(Adv_{D,UM} + Adv_{I,UM} + Ex_{UM,U}\right) = NewProd \tag{2}$$

For nitrate in the UM box,

$$\begin{aligned} &Adv_{D,UM}\ N_D + Adv_{I,UM} N_I + x\ NewProd = N_{UM}\left(Adv_{D,UM} + Adv_{I,UM}\right) \\ &\quad + Ex_{UM,U}(N_{UM} - N_U) + Ex_{D,UM}(N_{UM} - N_D) + Ex_{I,UM}(N_{UM} - N_I) \end{aligned} \tag{3}$$

where x is the proportion of $NewProd$ remineralized in the UM box. From equations 2 and 3, nitrate concentration in the UM box (N_{UM}) becomes

$$\begin{aligned} N_{UM} = \frac{\left(Adv_{D,UM} + Ex_{D,UM}\right)N_D + N_I(Adv_{I,UM} + Ex_{I,UM})}{\left(Adv_{D,UM} + Adv_{I,UM} + Ex_{UM,U} + Ex_{D,UM} + Ex_{I,UM}\right)} \\ - x(Adv_{D,UM} + Adv_{I,UM} + Ex_{UM,U}) \end{aligned} \tag{4}$$

For the oxygen balance in the UM box:

$$\begin{aligned} &Adv_{D,UM} O_D + Adv_{I,UM} O_I + Ex_{I,UM}(O_I - O_{UM}) + Ex_{D,UM}(O_D - O_{UM}) \\ &\quad + Ex_{D,UM}(O_U - O_{UM}) = \left(Adv_{D,UM} + Adv_{I,UM}\right)O_{UM} + r_a\ x\ NewProd \end{aligned} \tag{5}$$

where O_n is the oxygen concentration in the respective box, n, and r_a is the ratio between oxygen used and nitrate produced during organic matter mineralization (Table 1). Equations 2 and 5 are solved to yield an expression for oxygen in the UM box (O_{UM}):

$$\begin{aligned} O_{UM} = \frac{O_D\left(Adv_{D,UM} + Ex_{D,UM}\right) + O_I\left(Adv_{I,UM} + Ex_{I,UM}\right) + }{\left(Adv_{D,UM} + Adv_{I,UM} + Ex_{UM,U} + Ex_{D,UM} + Ex_{I,UM}\right)} \\ \frac{Ex_{UM,U}\ O_U - r_a\ x\ N_{UM}(Adv_{D,UM} + Adv_{I,UM} + Ex_{UM,U})}{\left(Adv_{D,UM} + Adv_{I,UM} + Ex_{UM,U} + Ex_{D,UM} + Ex_{I,UM}\right)} \end{aligned} \tag{6}$$

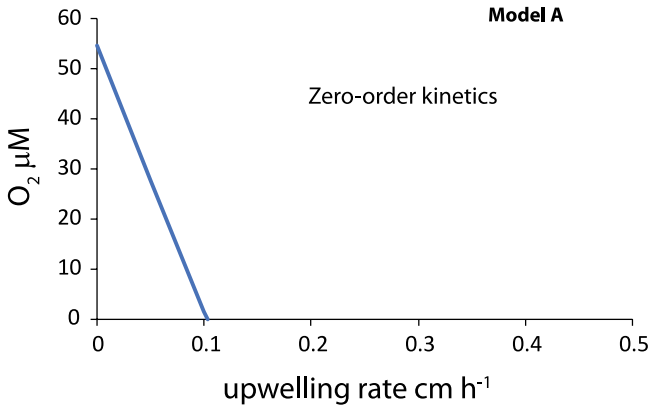

Figure 3. Results from Model A. Oxygen concentration in the *UM* box as a function of upwelling rate ($Adv_{D,UM}$; see Fig. 2) with zero-order respiration kinetics.

There is no oxygen-dependent control on oxygen respiration in this model and thus, oxygen is consumed with zero-order kinetics. From equation 6, we explore the relationship between O_{UM} and upwelling rate (we vary $Adv_{I,UM}$ to do this, keeping $Adv_{D,UM}$ equal to zero, although $Adv_{D,UM}$ could also be changed with similar results), which is a primary factor driving OMZ anoxia in this model construction (Canfield 2006). With model input parameters given in Table 1, we see (Fig. 3) that without any feedbacks (zero-order kinetics on oxygen respiration), there is a linear inverse relationship between O_{UM} and upwelling rate. Also, and critically, in this type of model, the maintenance of low-oxygen concentrations requires almost perfectly consistent rates of upwelling (as well as other mixing parameters) because only small changes would drive the system in and out of anoxia. Therefore, as described above, the maintenance of low-oxygen conditions in OMZ settings requires an oxygen-dependent control on carbon oxidation and thus oxygen consumption.

b. Oxygen control on oxygen respiration

As noted above, rates of oxic respiration typically become limited by oxygen at concentrations in the nanomolar to low micromolar range. Thus, one can view oxygen respiration as following Michaelis–Menten kinetics such that

$$Rate = \frac{Ratemax * O_2}{k_m + O_2} \tag{7}$$

where "*Rate*" is the rate of oxygen respiration, O_2 is the oxygen concentration, and k_m is the half-saturation constant at which the rate of oxygen respiration is at half its maximum value (*Ratemax*). Values of k_m are quite variable among aerobes and depend, to a large extent, on whether the organism utilizes a low-affinity (with a relatively high k_m value) or a high-affinity (with a relatively low k_m value) oxidase enzyme in their metabolism. In

Escherichia coli, which has both a high-affinity cytochrome *bd* oxidase and a low-affinity cytochrome *bo* oxidase, the k_m value for the low-affinity oxidase is in the range of 200 nM oxygen whereas the high-affinity oxidase has a k_m of 3 to 8 nM (Rice and Hempfling 1978). The k_m values for aerobes, however, can vary substantially from these values, and for a range of marine aerobes studied by Devol (1978), k_m values ranged from 760 to 4,200 nM. In another study of marine aerobes with both high- and low-affinity oxidase enzymes, k_m values ranged from 20 to 60 nM (Gong et al. 2016), and for natural microbial populations from a low-oxygen marine setting, an apparent k_m value of 391 ± 111 nM was determined (Garcia-Robledo et al. 2016), reflecting a composite of organisms with different k_ms. In our modelling, we will use a k_m value of 400 nM.

From a modelling perspective (see below), we explore 2 different types of kinetic control of aerobic respiration. The first follows standard Michaelis–Menten kinetics as expressed in equation 7. Such kinetics are standard in biogeochemical modeling of OM environments (Al Azhar et al. 2014; Gutknecht et al. 2013; Sankar et al. 2018; Penn et al. 2016; Anderson 2007), but, as we shall see below, they do not easily allow a transition from Bay of Bengal low-oxygen conditions to "functional" anoxia. Therefore, we also explore a model in which the organic matter pool decomposes with two types of kinetic control (Fig. 4a): one portion of the new production (y) decomposes with Michaelis–Menten control, and the other ($1 - y$) decomposes with no oxygen control (zero-order kinetics as an Model A). Equation 8 expresses these kinetics:

$$\left[\frac{O_{UM}}{k_m + O_{UM}}\right] xyNewProd + (1 - y)\, xNewProd \tag{8}$$

We could have alternatively modelled the second portion of decomposing organic matter with a Michaelis–Menten expression having an extremely low k_m value (e.g., Bristow et al. 2017). This would have the advantage of using a biologically understood expression of oxygen control. However, "functional" anoxia would only be achieved if we set k_m to an oxygen concentration below where we believe "functional" anoxia begins. If we did so, model results would be nearly identical to what we produce with a zero-order kinetics on oxygen respiration. However, we do not precisely know the oxygen level of "functional" anoxia and by using zero-order kinetics we make no assumptions as to what this oxygen concentration might be. We have, therefore, elected to use zero-order kinetics for the second portion of the decomposing organic matter. We reiterate, however, that there is very little difference between using this approach and that of a dual Michaelis–Menten approach utilizing both high and low k_m values.

We appreciate that a zero-order control on organic matter decomposition does not have an obvious biological underpinning. As noted above, we can view this portion of organic matter as oxidizing with an extremely low, but currently undefined, k_m value. Zero order–like kinetics could also represent oxygen utilization by additional processes such as the aerobic oxidation of reduced products of anaerobic metabolism (occurring concurrently with the aerobic oxidation of organic matter under low oxygen concentrations; e.g., Bristow et al.

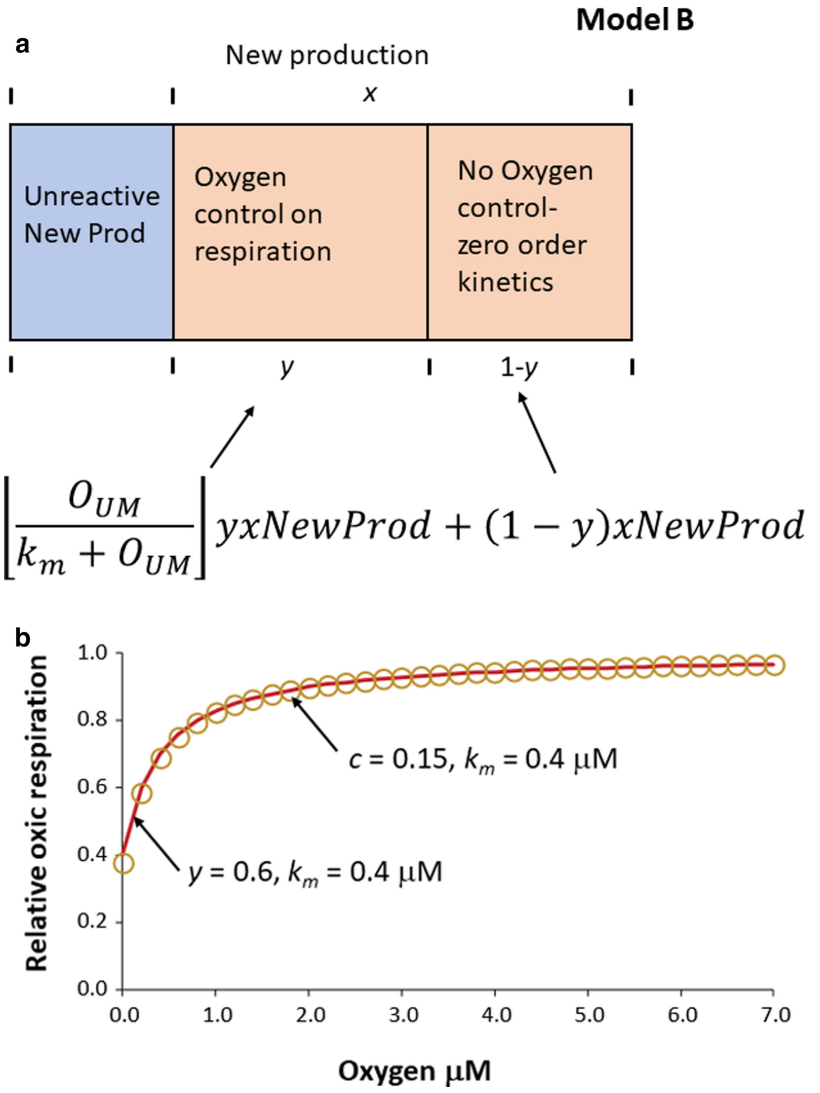

Figure 4. Description of Model B. (a) model with oxygen dependent oxic respiration. Here, x represents the amount of new production metabolized in the *UM* box in Figure 2, y represents the amount of this new production that is oxidized by aerobic respiration with Michaelis–Menten kinetics, and $(1-y)$ represents the fraction metabolized with zero-order kinetics. The parts of the kinetic control equations representing the different types of oxygen control in oxygen respiration are indicated. (b) the relative rates of oxic respiration as a function of oxygen concentration. Two model results are shown: one a mixture of Michaelis–Menten with zero-order kinetics (y = 0.6, *km* of 400 nM) (red line), as in equation 8, and the other with a Michaelis–Menten and hyperbolic kinetics (c = 0.15, *km* of 400 nM) (open circles), as in equation 9. See text for details.

2017; Lam et al. 2011), such as nitrite, or fermentation products like H_2 or fatty acids, each with their own very low k_m values. The resulting kinetic expression for a k_m of 400 nM and y of 0.6 (60% of the decomposing organic matter under Michaelis–Menten control) is shown in Figure 4(b).

We note that other kinetic expressions can produce a similar functional form to that shown in Figure 4(b). For example, the Michaelis–Menten expression can be modified to the following form:

$$Rate = \frac{Ratemax * (O_2 + C)}{k_m + O_2} \tag{9}$$

and with $C = 0.15$, an identical kinetic expression is produced to that described above and as shown in Figure 4(b). In this case, respiration could be viewed as occurring with 2 kinetic controls: one control is normal Michaelis–Menten kinetics as expressed in equation 5, and the other would be an increasing (with decreasing oxygen) hyperbolic function ($Rate = Ratemax*C/(k_m + O_2)$, with a finite and maximum respiration rate at zero oxygen concentration. Although this expression would produce the same kinetic functionality to that from equation 8, we can think of no physiological explanation for the increasing hyperbolic function and the resulting high metabolic rates at zero oxygen concentration. Therefore, we have elected not to pursue this functionality for the oxygen control of aerobic respiration.

Given the above considerations, we write mass balance equations for nitrogen (equation 10) and oxygen (equation 11) in the *UM* box and assume, as before, that N_U is zero:

$$\begin{aligned} &Adv_{D,UM}\ N_D + Adv_{I,UM}\ N_i + \left[\frac{O_{UM}}{k_m + O_{UM}}\right] x\ y\ NewProd + (1-y)x\ NewProd \\ &\quad = \left(Adv_{D,UM} + Adv_{I,UM}\right)N_{UM} + Ex_{D,UM}(N_{UM} - N_D) \\ &\qquad + Ex_{I,UM}(N_{UM} - N_I) + Ex_{UM,U}(N_{UM}) \end{aligned} \tag{10}$$

$$\begin{aligned} &Adv_{D,UM}\ O_D + Adv_{I,UM}\ O_I + Ex_{D,UM}(O_D - O_{UM}) + Ex_{I,UM}(O_I - O_{UM}) \\ &\quad + Ex_{UM,U}(O_U - O_{UM}) = \left(Adv_{D,UM} + Adv_{I,UM}\right)O_{UM} \\ &\quad + r_a\ x\ y\left[\frac{O_{UM}}{k_m + O_{UM}}\right]NewProd + r_a\ x\ (1-y)\ NewProd. \end{aligned} \tag{11}$$

We could find no analytical solution for these equations and have therefore used the Excel solver® function to find values for N_{UM}, O_{UM}, and *NewProd* from equations 2, 10, and 11 with the mixing and concentration input parameters in Table 1 (and as also used above), with variable upwelling rate ($Adv_{I,UM}$) and with different values of y.

We begin by exploring the model results for organic matter decomposition with Michaelis–Menten kinetics alone ($y = 1$). With values of k_m of $\leq$100 nM, we reproduce oxygen concentrations in the range found in the Bay of Bengal and over a broad range of upwelling rates (Fig. 5a and b). Thus, these results would seemingly be compatible with

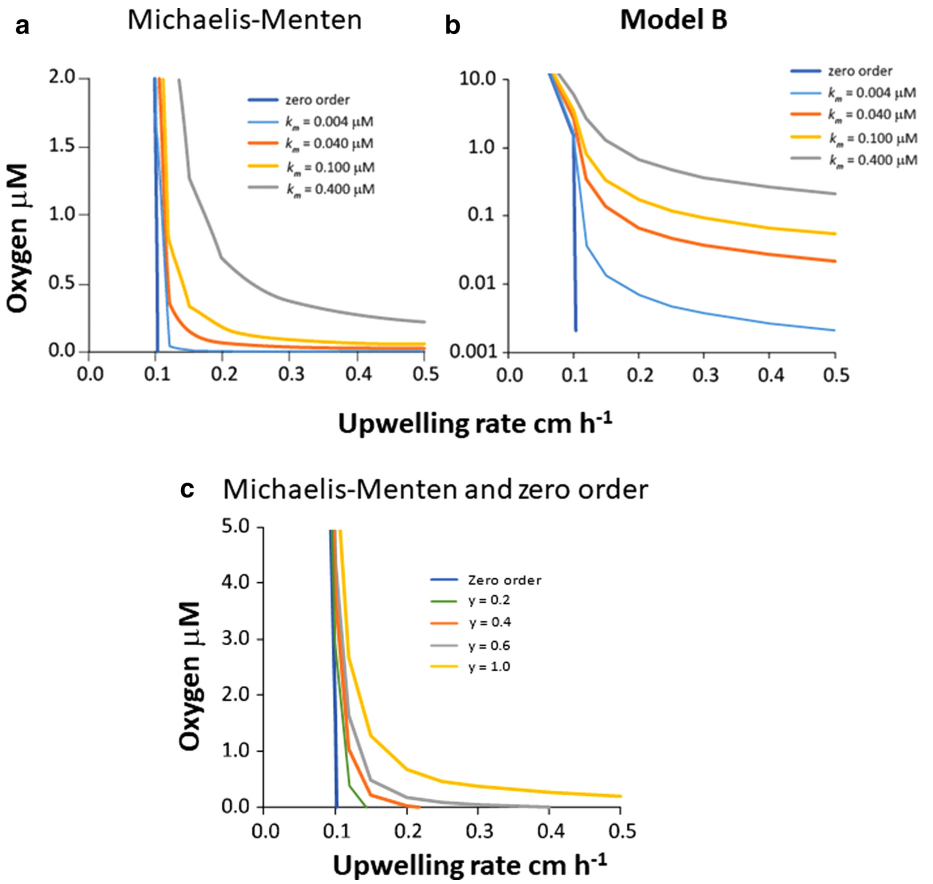

Figure 5. Results from model B. (a) model results with only Michaelis–Menten control on oxygen respiration as a function of upwelling rate and with variable values of k_m. (b) same as in (a), but with oxygen plotted on log scale. (c) model results with both Michaelis and in and zero-order control on oxygen respiration. y represents the fraction of decomposing organic matter oxidizing with Michaelis–Menten kinetics. The remainder of the decomposing organic matter $(1 - y)$ oxidizes with zero-order control on oxygen concentration. The value of k_m is 0.4 µM.

field observations from the Bay of Bengal (Bristow et al. 2017). However, "functional" anoxia (in our estimation oxygen concentrations in the sub-nM range) is not achieved with this model unless the *km* value is also in the low nM range (Fig. 5a and b). Such low values for k_m are much lower than those reported for aerobic respiration by OMZ microbes (Garcia-Robledo et al. 2016), and, furthermore, Bay of Bengal oxygen concentrations are not attained except over a very narrow range of upwelling rates, similar to the situation with just zero-order kinetics controlling oxygen respiration (Model A; Fig. 3). Therefore, the single-k_m model cannot reproduce both the oxygen levels as found in the Bay of Bengal and a transition to "functional" anoxia as occurs in the ODZs of the world's ocean. For this

reason, a single-k_m model is viewed as an inappropriate representation of oxygen respiration in the Bay of Bengal and probably also other OMZ environments.

When a portion of new production is oxidized with zero-order kinetics, oxygen concentrations in the *UM* box can be maintained to Bay of Bengal–like concentrations over a broad range of upwelling rates. The pseudostabilization of oxygen over a broad range of upwelling rates becomes more prominent with higher values of y, but if $y = 1$, meaning that all decomposing new production is oxidized with Michaelis–Menten kinetics (as described above), oxygen never reaches zero (Fig. 5; $k_m = 0.4\ \mu$M). Therefore, we must introduce the oxidation of some organic matter with zero order–like kinetics to allow OMZs to eventually become "functionally" anoxic. We could also explore the influence of changing other input parameters such as concentrations of nutrients and oxygen in the D, U, and I boxes, as well as other mixing parameters, but our goal here is not to "best fit" available data. Rather, we seek to explore how an oxygen feedback on organic matter mineralization can act to stabilize oxygen levels to low values in an OMZ setting.

c. Oxygen inhibition of denitrification

Two anaerobic processes produce N_2 in OMZ settings, and both are inhibited by oxygen, but in different ways. As noted above, although many denitrifiers can produce N_2 in the presence of oxygen (Chen and Strous 2013), there can be a physiological control on denitrification rates such that in natural settings, denitrification becomes inhibited as oxygen concentrations increase (Bristow et al. 2017; Dalsgaard et al. 2014). Anammox ($NO_2^- + NH_4^+ \rightarrow N_2 + H_2O$; van de Graaf et al. 1995; Strous et al. 1999) is also inhibited by oxygen, but in two different ways. First, there is a direct physiological inhibition. Thus, whereas anammox can occur in weakly oxygenated settings, the process becomes completely inhibited as oxygen increases to between 2 and 20 μM (Dalsgaard et al. 2014; Jensen et al. 2008; Kalvelage et al. 2011). Second, and as noted above, nitrification efficiently removes nitrite from even weakly oxygenated water columns including the Bay of Bengal OMZ (Bristow et al. 2017; Thamdrup et al. 2012). Thus, for the Bay of Bengal, even though the low oxygen levels measured would seemingly allow the anammox process to occur (indeed, anammox bacteria are found in these waters), the lack of nitrite in the water column due to nitrification substantially suppresses anammox activity (Bristow et al. 2017). Therefore, because of the lack of nitrite in low-oxygen (but not functionally anoxic) settings, we will focus on the oxygen inhibition of denitrification as the primary process in the nitrogen cycle providing a negative feedback on oxygen utilization.

Following the above discussion, denitrification can be defined by an inhibition expression (Dalsgaard et al. 2014) in which, in the present model context, rates of denitrification are given as follows:

$$denitrf = \left(1 - \left[\frac{O_{UM}}{k_{mn} + O_{UM}}\right]\right) z\ x\ NewProd \tag{12}$$

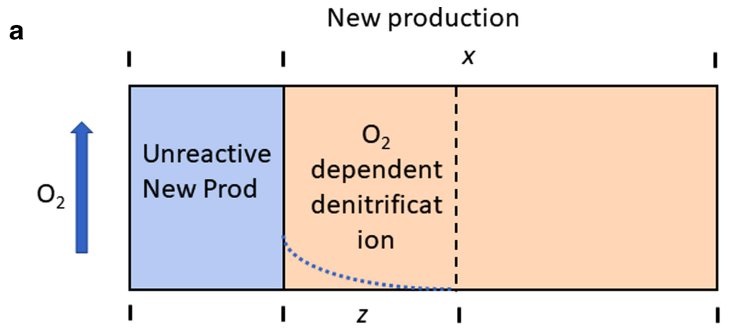

$$\text{"denitrif"} = zxNewProd - \left\lfloor \frac{O_{UM}}{k_m + O_{UM}} \right\rfloor zxNewProd$$

$$\text{oxic resp} = xNewProd\text{-}(zxNewProd - \left\lfloor \frac{O_{UM}}{k_{mn} + O_{UM}} \right\rfloor zxNewProd)$$

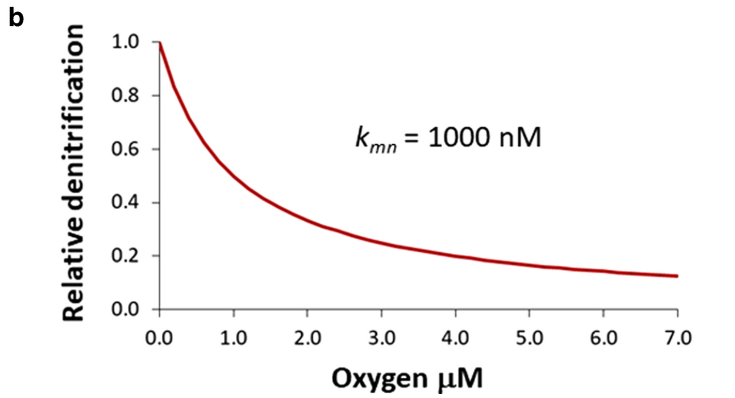

Figure 6. (a) model with oxygen-dependent denitrification. Here, x represents the amount of new production metabolized in the *UM* box in Figure 2 and z represents the amount of this new production that is subject to oxygen-dependent denitrification. The organic matter available for oxidation (x) and not oxidized by denitrification is oxidized by oxic respiration with zero-order kinetics. The blue dotted line shows that within the z fraction of organic matter, the amount actually oxidized by denitrification increases as oxygen level decreases. (b) plot showing how the relative rates of denitrification are controlled as a function on oxygen concentration with an inhibition constant, k_{mn}, of 1,000 nM.

In addition to the parameters already defined, z is the proportion of the new production undergoing decomposition in the *UM* box that is also susceptible to decomposition by denitrification ($z \leq x$), and k_{mn} is the one-half inhibition constant of oxygen for denitrification (see Fig. 6a and b). The organic matter available for respiration in the *UM* box (*xNewProd*),

and not oxidized by denitrification, is oxidized by aerobic respiration with no oxygen control (zero-order kinetics) and is expressed by

$$Oxic\ resp = x\ NewProd - \left(1 - \left[\frac{O_{UM}}{k_{mn} + O_{UM}}\right]\right) z\ x\ NewProd \tag{13}$$

With these relationships, mass balance equations are written for N_{UM} (equation 14) and O_{UM} (equation 15) in the *UM* box:

$$\begin{aligned} &Adv_{D,UM}\ N_D + Adv_{I,UM}\ N_i + xNewProd = (Adv_{D,UM} + Adv_{I,UM})N_{UM} \\ &\quad + Ex_{UM,U}N_{UM} + Ex_{D,UM}N_{UM} - Ex_{D,UM}N_D + Ex_{I,UM}N_{UM} \\ &\quad - Ex_{I,UM}N_I + \left(1 - \left[\frac{O_{UM}}{k_{mn} + O_{UM}}\right]\right) zx\ r_n\ NewProd \end{aligned} \tag{14}$$

$$\begin{aligned} &Adv_{D,UM}O_D + Adv_{I,UM}O_I + Ex_{D,UM}(O_D - O_{UM}) + Ex_{I,UM}(O_I - O_{UM}) \\ &\quad + Ex_{UM,U}(O_U - O_{UM}) = (Adv_{D,UM} + Adv_{I,UM})O_{UM} \\ &\quad + r_a\ x\ NewProd - \left(1 - \left[\frac{O_{UM}}{k_{mn} + O_{UM}}\right]\right) r_a\ z\ x\ NewProd) \end{aligned} \tag{15}$$

where, in addition to terms already defined, r_n (with a value of 5.9) is the ratio between N liberated as N_2 during carbon oxidation by denitrification compared to the N liberated during oxic respiration. For OMZ waters off the northern coast of Chile, an inhibition constant for denitrification, k_{mn}, of about 300 nM was determined (Dalsgaard et al. 2014), whereas for waters of the Bay of Bengal, the k_{mn} seems to be closer to 1,000 nM (Bristow et al. 2017). A k_{mn} value of 1,000 μM will be used in our modelling. Again, we found no analytical solutions to these equations, so Excel solver® was used to find values for N_{UM}, O_{UM}, and *NewProd* from equations 2, 14, and 15 with variable rates of upwelling ($Adv_{I,UM}$) and for different values for z. Other parameters were as given in Table 1.

The oxygen control of denitrification in the low-oxygen waters generates a very strong feedback on oxygen persistence in the model results (Fig. 7). This is because denitrification diverts mineralization from oxic respiration and, through N_2 production, generates a strong limitation on nitrate availability that feedbacks into primary production and thus the settling rate of organic matter (*NewProd*) into the *UM* box. As with the oxygen control on oxygen respiration, if all the organic matter is potentially oxidized by denitrification with an inhibition as expressed in equation 12, oxygen will never be fully utilized and functional anoxia will not occur. Indeed, as before, to achieve functional anoxia, some of the organic matter must decompose by aerobic respiration with zero-order like oxygen control on the decomposition rate. At intermediate values of z, oxygen can persist at low concentrations through quite a range of upwelling rates. Thus, the oxygen inhibition of denitrification represents a potentially powerful feedback regulating oxygen concentrations to low values in OMZ waters.

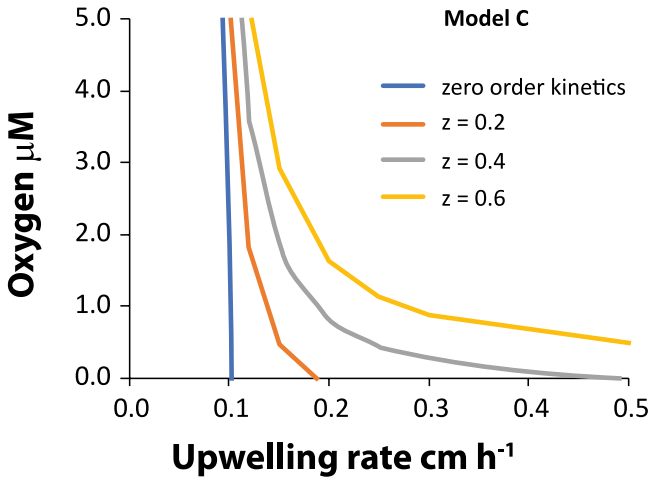

Figure 7. Results from model with oxygen control on denitrification with variable values of z, representing the fraction of decomposing organic matter influenced by an oxygen inhibition of denitrification. See text for details.

d. Oxygen control on oxygen respiration and an oxygen inhibition of denitrification

It seems quite probable that the oxygen regulation of both denitrification and oxic respiration are active in low-oxygen waters, because, as noted above, each of these types of regulation have been identified in OMZ environments. Therefore, we explore how both feedbacks operating together can combine to regulate oxygen to low concentrations in OMZ settings. In doing so, as with the oxygen dependence on oxic respiration (Fig. 4), we divide the amount of new production available for oxidation in the *UM* box into two fractions: the fraction y, representing the organic matter decomposing in the *UM* box (*xNewProd*) undergoing oxygen-dependent respiration (both oxic respiration and denitrification), and the fraction $1 - y$ representing the organic matter undergoing oxygen-independent oxic respiration. Of the organic matter undergoing oxygen-dependent respiration, some fraction, z, is susceptible to denitrification and subject to oxygen inhibition (Figs. 6 and 8). Thus, rates of denitrification (*denitrif*) are written as:

$$denitrif = xyzNewProd - \left[\frac{O_{UM}}{k_{mn} + O_{UM}} xyzNewProd\right] \tag{16}$$

The total rate of oxic respiration (*Oxic resp*) includes the sum of oxygen-dependent and oxygen-independent fractions and is given as follows:

$$Oxic\ resp = r_a \left(\left[\frac{O_{UM}}{k_m + O_{UM}}\right](xyNewProd - denitrif) + (1 - y)\, xNewProd\right) \tag{17}$$

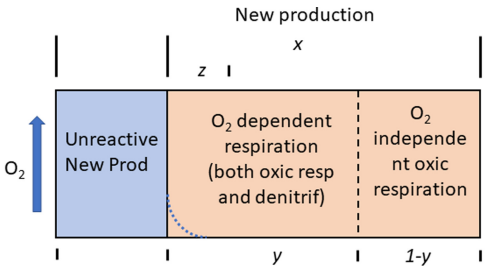

$$\text{"denitrif"} = zyxNewProd - \left[\frac{O_{UM}}{k_{mn}+O_{UM}}\right] zyxNewProd$$

$$\text{oxic resp} = \left[\frac{O_{UM}}{k_m+O_{UM}}\right] (xyNewProd - denitrif) + (1-y)xNewProd$$

(O_2 dependent; O_2 independent)

Figure 8. Model with oxygen dependency on both oxic respiration and denitrification. y is the proportion of organic matter decomposing in the *UM* box that undergoes oxygen-dependent mineralization. z is the proportion of this organic matter subject to oxgen control. The proportion of y not decomposing by denitrification is subect to oxygen-dependent oxic respiration. The dotted blue line shows how the organic matter within the "z" pool is subject to increasing amounts of denitrification as oxygen levels decrease. The equations expressing these functionalities are also shown. See text for details.

From these expressions, and with $N_U = 0$, we write mass balance equations for oxygen in the *UM* box, O_{UM} (equation 18), and nitrate in the *UM* box, N_{UM} (equation 19):

$$\begin{aligned} &Adv_{D,UM} N_D + Adv_{I,UM} N_i + (1-y)\, xNewProd \\ &+ \left[\frac{O_{UM}}{k_m + O_{UM}}\right]\left[xyNewProd - xyzNewProd + xyzNewProd\frac{O_{UM}}{k_{mn} + O_{UM}}\right] \\ &+ xyzNewProd - xyzNewProd\frac{O_{UM}}{k_m + O_{UM}} = \left(Adv_{D,UM} + Adv_{I,UM}\right) N_{UM} \\ &+ Ex_{UM}(N_{UM} - N_D) + Ex_{I,UM}(N_{UM} - N_I) + Ex_{UM,U}(N_{UM}) \\ &+ r_n xyzNewProd - r_n xyzNewProd\frac{O_{UM}}{k_{mn} + O_{UMK}} \end{aligned} \tag{18}$$

$$\begin{aligned} &Adv_{D,UM} O_D + Adv_{I,UM} O_I + Ex_{D,UM}(O_D - O_{UM}) + Ex_{I,UM}(O_I - O_{UM}) \\ &+ Ex_{UM,U}(O_U - O_{UM}) = \left(Adv_{D,UM} + Adv_{I,UM}\right) O_{UM} \\ &+ r_a\,(1-y)\, xNewProd + r_a\left[\frac{O_{UM}}{k_m + O_{UM}}\right] \\ &\times \left[xyNewProd - xyzNewProd + xyzNewProd\frac{O_{UM}}{k_{mn} + O_{UM}}\right] \end{aligned} \tag{19}$$

Using Excel solver, equations 2, 18, and 19 were solved for values of O_{UM}, N_{UM}, and *NewProd* with input parameters in Table 1 and with variable choices for y and z. The results are compared to the results from Models B and C in Figure 9. When combined, these two feedbacks generate similar model results to those produced when each feedback was considered individually.

4. Discussion

Our results show that working both independently and together, both an oxygen control on oxic respiration and an oxygen inhibition of denitrification can contribute to the persistence of low-oxygen conditions in OMZ settings subject to upwelling. We note, however, that each of these control mechanisms operates in fundamentally different ways. Thus, if oxygen controls rates of oxic respiration in the OMZ, there is little influence on the rate of net primary production in the system (Fig. 10a) but a large influence on the proportion of the net primary production that is mineralized within the OMZ (Fig. 10b). The idea that carbon mineralization rate is reduced as organic matter settles through oxygen-depleted or nearly depleted OMZ waters is broadly consistent with studies showing that organic matter remineralization through OMZ can be reduced by about 50% compared to organic matter settling through well-oxygenated water columns (Cavan et al. 2017; Devol and Hartnett 2001; Keil et al. 2016; Van Mooy et al. 2002).

It is currently uncertain, however, whether the reduction in carbon mineralization in water columns with reduced oxygen concentration is due to a direct oxygen influence on organic matter mineralization or to differences in how secondary consumers process and disaggregate organic detritus in the different environments (Cavan et al. 2017). With respect to grazers, the idea is that under oxygenated conditions, grazing zooplankton disaggregate settling organic aggregates, enhancing their decomposition (Cavan et al. 2017). It is not yet known whether grazing zooplankton are active in very low-oxygen environments like the Bay of Bengal. Also, although the Bay of Bengal OMZ is not completely analogous to some of the ODZ environments in which many sediment-trap experiments have been performed, the influence of oxygen on rates of aerobic microbial metabolism makes sense given how aerobic metabolism responds to oxygen concentration in cultures of microbial aerobes, as well as in nature, as explored above.

The strength of our oxygen feedback on aerobic respiration depends, mainly, on the balance between the proportion of new production that decomposes with an oxygen dependence and the proportion that decomposes with zero-order kinetics (Fig. 7). As mentioned above, the proportion of new production decomposing with zero-order kinetics may, in fact, represent a variety of processes including the reoxidation of the reduced products of anaerobic metabolism with very low k_m values as well as a fraction of organic matter that might consume oxygen with something approaching zero-order kinetics or with kinetics expressing very low k_m values. It is clear, however, that without some zero-order

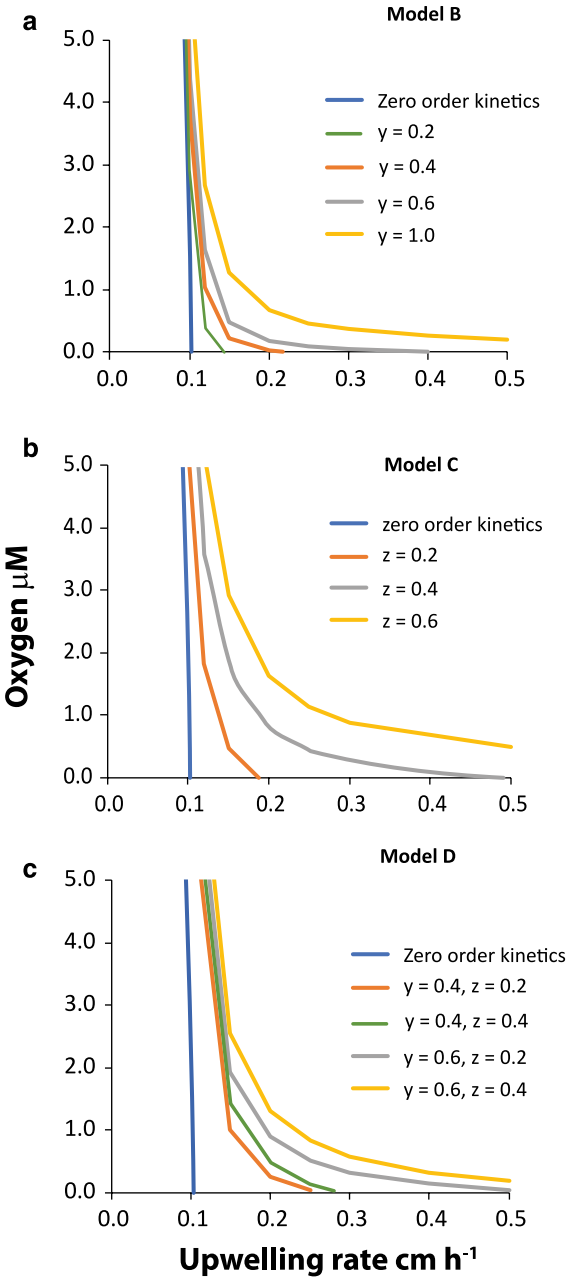

Figure 9. (a) results for oxygen control on oxic respiration (Model B) reproduced from Figure 5. (b) results with oxygen control on denitrification (Model C) reproduced from Figure 7. (c) results for oxygen control on both oxic respiration and denitrification with variable values for y and z (Model D). See text and Figure 8 for details.

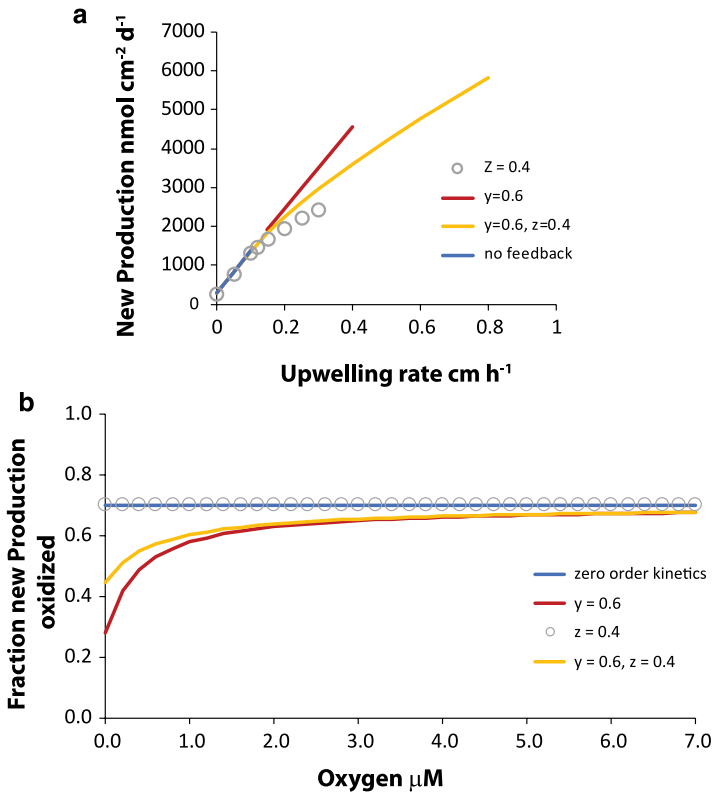

Figure 10. (a) rates of new production in a selection of models with oxygen control on denitrification and oxic respiration. (b) fraction of new production oxidized in a selection of models with oxygen control on denitrification and oxic respiration. In these models the value of $x = 0.7$. See text for details.

control on oxygen utilization (or something like it), OMZs would not become functionally anoxic. Therefore, although our proportioning between new production decomposing with oxygen-control and that decomposing with zero-order kinetics is a model construct, the incorporation of two types of oxygen regulation is required to explain the attainment of ODZs. The value of y, however, which describes the magnitude of the proportioning, is a free variable that could potentially be constrained through careful modelling of real-world low–oxygen environments.

The oxygen control on denitrification represents a fundamentally different type of oxygen-regulation mechanism. In this case, rates of denitrification increase as oxygen concentrations decrease, reducing nitrogen availability and thus directly influencing new production rate (Fig. 10a). This feedback working alone, however, does not influence the fraction of new production oxidized in the OMZ waters (Fig. 10b). The oxygen-dependent denitrification feedback is a strong feedback, and, as noted above, if all the new production

was susceptible to denitrification under oxygen control, then an ODZ would never develop. Therefore, and as with a feedback expressing oxygen control of oxic respiration, some of the new production must decompose aerobically with something like zero-order oxygen kinetics. Also, the value of z, describing the proportion of organic matter subject to denitrification, is a free parameter that could potentially be set by modeling real-world low–oxygen environments.

The most realistic oxygen-control model is probably the one that incorporates both an oxygen control on aerobic respiration and an oxygen control on denitrification. This model also generates a very strong feedback in regulating oxygen to low concentrations, but the feedback seems to be of similar strength to the two oxygen-control mechanisms operating independently (Fig. 10). To attain functional anoxia with these two feedbacks working together, it is also required that one pool of new production is subject to an oxygen control on metabolism, whereas another pool decomposes with zero-order kinetics on oxygen consumption. Also, as with the other models, values of y and z could potentially be constrained through modeling of real-world low–oxygen OMZs.

Both mechanisms of oxygen control explored here are plausible on the basis of what is understood about the regulation of oxygen concentration on aerobic respiration and on denitrification in nature, Also, these oxygen feedbacks likely act to stabilize oxygen to low concentrations in the Bay of Bengal and possibly other marine low-oxygen environments such as, for example, the Pescadero Basin and the outer reaches of otherwise ODZs. Indeed, Penn et al. (2016) have reached a somewhat similar conclusion arguing that the kinetics of oxic respiration influence the extent of oxygenated waters in OMZ settings. This paper, however, was not aimed at trying to explore the mechanisms potentially stabilizing low-oxygen conditions.

We emphasize that the relative persistence of low-oxygen conditions is a semistable situation and that significant changes in rates of upwelling or other mixing parameters can flip a system between oxic and functionally anoxic states. Such flips may be the case in the Bay of Bengal, in which microbial populations are similar to those found in ODZs, yet, especially for anammox (Bristow et al. 2017), rates are significantly inhibited owing to lack of nitrite in the low-oxygen waters. Periodic increases in rates of upwelling, for example, could encourage extreme oxygen depletion in some places of the Bay of Bengal, acting to satiate the anaerobic microbial populations.

Our results are also compatible with the idea that the persistence of low-oxygen conditions in the Bay of Bengal, as compared with ODZ conditions in the Arabian Sea, could have an origin in the ballasting and, thus, rapid sinking of net production by river particles from the Ganges and Brahmaputra rivers (Al Azhar et al. 2017; Lutz et al. 2002; Rao et al. 1994). In our model, such ballasting would have the effect of decreasing the value of x, and we see in Figure 11 that with the same oxygen controls in place, reducing the value of x can drive a system from anoxia to weakly oxygenated conditions at the same rate of upwelling. Therefore, such a difference in ballasting between the Arabian Sea and the Bay of Bengal would be completely consistent with our modeling structure.

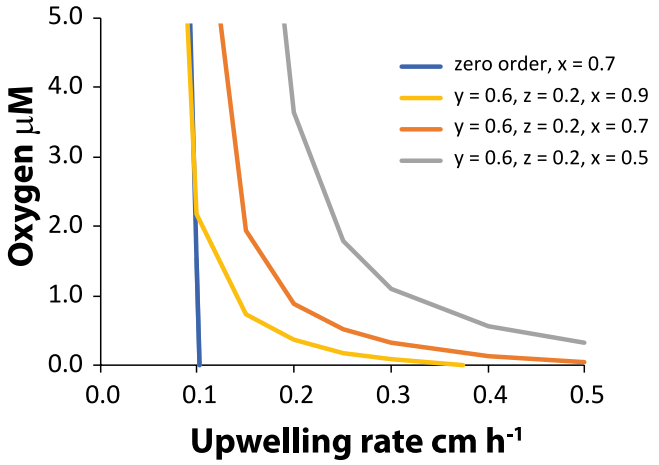

Figure 11. Model results with feedbacks on oxic respiration and denitrification and changing x, the proportion of new production available for decomposition in the *UM* box.

As this is a conceptual model exercise, we have not invested great energy in trying to fit the oxygen biogeochemistry of any particular low-oxygen setting. We feel that a regional ocean modeling exercise would be better suited to this, and such a model would also be better suited to choosing values for the free variables we have in our model construction. Nevertheless, we find that average rates of oxic respiration in the low-oxygen portion of the Bay of Bengal are consistent with the range of values derived from our model (Fig. 12a). The low estimates for the Bay of Bengal (14 n moles C oxidized l^{-1} d^{-1}) are derived from comparing the integrated ETS activity in the Bay of Bengal with that of the Arabian Sea, in which the Arabian Sea value has been calibrated to rates of carbon oxidation in the ODZ waters (Naqvi et al. 1996) and the higher rates (63 n moles C oxidized l^{-1} d^{-1}; not shown on the figure) are from Al Azhar et al. (2017).

We also compare our modelled rates of denitrification to rates measured in oxygen-control experiments from the from Bay of Bengal OMZ waters (for O_2 concentrations below 1 μM; Fig. 12b) as well as with rates of nitrate reduction to nitrite in Bay of Bengal waters (Bristow et al. 2017). The latter can be taken as a measure of the maximum potential rate denitrification, as this is the first step in the denitrification process. With the chosen values of model parameters, the model reproduces measured denitrification rates at upwelling rates between 0.1 and 0.15 cm h^{-1} and measured nitrate reduction rates at upwelling rates of between 0.18 to 0.35 cm h^{-1}. Within this range of upwelling rates, the model displays oxygen control on oxygen depletion, especially at upwelling rates of over 0.2 cm h^{-1} (Fig. 9). Therefore, as our model is set up, and without special tuning, model results approximate the carbon, nitrogen, and oxygen cycles of the Bay of Bengal OMZ over a range of upwelling rates.

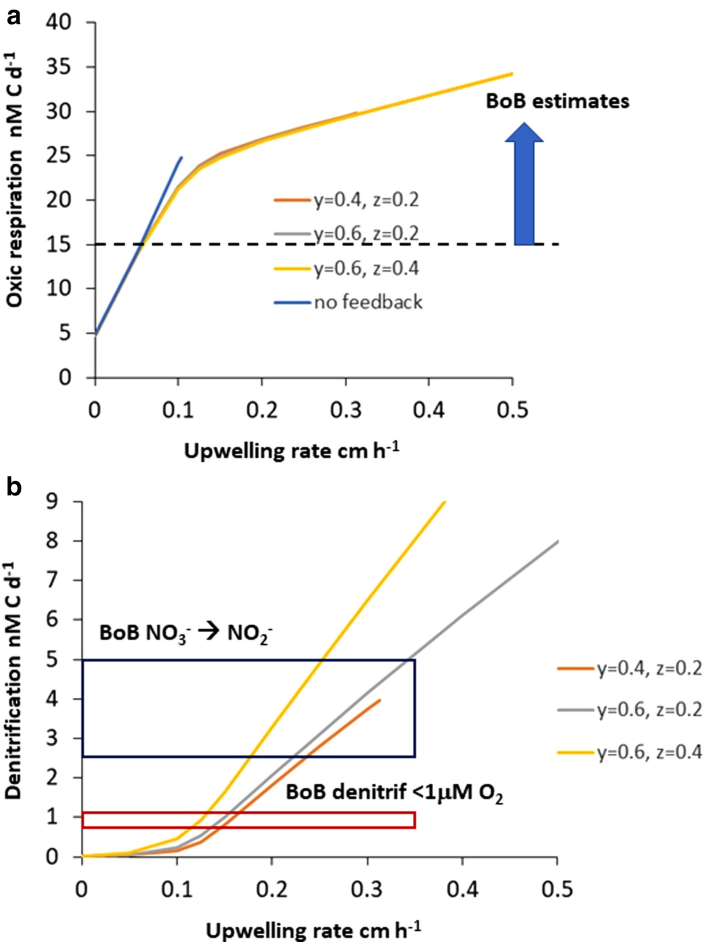

Figure 12. (a) average rates of oxic respiration in *UM* box with model runs using oxygen control on oxic respiration and denitrification. Estimates from the Bay of Bengal are shown for comparison. (b) average rates of denitrification in *UM* box with model runs using oxygen control on oxic respiration and denitrification. Measured rates of dentrification from the Bay of Bengal oxygen-minimum zone (OMZ) from oxygen control experiments of O_2 concentrations of <1 µM (Bristow et al. 2017). Also shown are measured rates of nitrate reduction to nitrite in Bay of bengal OMZ waters.

5. Conclusions

Low-oxygen conditions are found as semipersistent in the Bay of Bengal and likely many other regions of the global ocean, including the outer margins of otherwise functionally anoxic OMZs. With climate change, these low-oxygen regions will likely spread, some of them becoming anoxic themselves. The maintenance of low-oxygen conditions, as

well as their eventual transition to anoxia, is likely controlled by a balance between physical forcing processes and biological feedbacks. We show here that oxygen feedbacks on both aerobic respiration and denitrification can provide such feedbacks. In model simulations, these feedbacks reproduce semistable low-oxygen conditions over a range of physical forcing parameters. These feedbacks, when working together, influence both the rates of new production and the transport efficiency of the new production through the low-oxygen waters. Thus, these feedbacks have important implications for the carbon cycle. Aspects of these feedbacks have already been introduced into some regional ocean models with biogeochemical capabilities. However, we believe that carefully considering the nature of these feedbacks, and the parameters that control them, will help generate better models to more faithfully predict the distributions of low-oxygen waters today and the eventual spread of these waters in the future.

REFERENCES

Al Azhar, M., D. E. Canfield, K. Fennel, B. Thamdrup, and C. J. Bjerrum. 2014. A model-based insight into the coupling of nitrogen and sulfur cycles in a coastal upwelling system. J. Geophys. Res. Biogeosci., *119*(3), 264–285. doi: 10.1002/2012jg002271

Al Azhar, M., Z. Lachkar, M. Lévy, and S. Smith. 2017. Oxygen minimum zone contrasts between the Arabian Sea and the Bay of Bengal implied by differences in remineralization depth. Geophys. Res. Lett., *44*(21), 11106–11114. doi: 10.1002/2017GL075157

Anderson, T. R. 2007. Denitrification in the Arabian Sea: a 3D ecosystem modelling study. Deep Sea Res., *54*(12), 2082–2119. doi: 10.1016/j.dsr.2007.09.005

Babbin, A. R., R. G. Keil, A. H. Devol, and B. B. Ward. 2014. Organic matter stoichiometry, flux, and oxygen control nitrogen loss in the ocean. Science, *344*(6182), 406–408. doi: 10.1126/science.1248364

Bristow, L. A., C. M. Callbeck, M. Larsen, M. A. Altabet, J. Dekaezemacker, M. Forth, M. Gauns, et al. 2017. N_2 production rates limited by nitrite availability in the Bay of Bengal oxygen minimum zone. Nat. Geosci., *10*(1), 24–29. doi: 10.1038/ngeo2847

Bristow, L. A., T. Dalsgaard, L. Tiano, D. B. Mills, A. Bertagnolli, J. J. Wright, S. J. Hallam, et al. 2016. Ammonium and nitrite oxidation at nanomolar oxygen concentrations in oxygen minimum zone waters. Proc. Natl. Acad. Sci. U. S. A., *113*(38), 10601–10606. doi: 10.1073/pnas.1600359113

Broecker, W. S. 1974. Chemical oceanography. New York: Harcourt Brace Jovanovich. pp. 1–214.

Broecker, W. S., and T.-H. Peng. 1982. Tracers in the Sea. Palisades: Eldigio Press. pp. 1–690.

Canfield, D. E. 2006. Models of oxic respiration, denitrification and sulfate reduction in zones of coastal upwelling. Geochim. Cosmochim. Acta, *70*(23), 5753–5765. doi: 10.1016/j.gca.2006.07.023

Cavan, E. L., M. Trimmer, F. Shelley, and R. Sanders. 2017. Remineralization of particulate organic carbon in an ocean oxygen minimum zone. Nat. Commun., *8*, 14847. doi: 10.1038/ncomms14847

Chen, J. W., and M. Strous. 2013. Denitrification and aerobic respiration, hybrid electron transport chains and co-evolution. Biochim. Biophys. Acta Bioenerg., *1827*(2), 136–144. doi: 10.1016/j.bbabio.2012.10.002

Chronopoulou, P.-M., F. Shelley, W. J. Pritchard, S. T. Maanoja, and M. Trimmer. 2017. Origin and fate of methane in the Eastern Tropical North Pacific oxygen minimum zone. ISME J., *11*(6), 1386–1399. doi: 10.1038/ismej.2017.6

Cline, J. D., and I. R. Kaplan. 1975. Isotopic fractionation of dissolved nitrate during denitrification in the eastern tropical North Pacific Ocean. Mar. Chem., *3*(4), 271–299. doi: 10.1016/0304-4203(75)90009-2

Codispoti, L. A., and T. T. Packard. 1980. Denitrification rates in the eastern tropical South Pacific. J. Mar. Res., *38*(3), 453–477.

Dalsgaard, T., F. J. Stewart, B. Thamdrup, L. De Brabandere, N. P. Revsbech, O. Ulloa, D. E. Canfield, and E. F. DeLong. 2014. Oxygen at nanomolar levels reversibly suppresses process rates and gene expression in anammox and denitrification in the oxygen minimum zone off Northern Chile. Mbio, *5*(6), e01966. doi: 10.1128/mBio.01966-14

Devol, A. H. 1978. Bacterial oxygen uptake kinetics as related to biological processes in oxygen deficient zones of the oceans. Deep Sea Res., *25*(2), 137–146. doi: 10.1016/0146-6291(78)90001-2

Devol, A. H., and H. E. Hartnett. 2001. Role of the oxygen-deficient zone in transfer of organic carbon to the deep ocean. Limnol. Oceanogr., *46*(7), 1684–1690. doi: 10.4319/lo.2001.46.7.1684

Fernandez, C., L. Farias, and O. Ulloa. 2011. Nitrogen fixation in denitrified marine waters. PLoS One, *6*(6), e20539. doi: 10.1371/journal.pone.0020539

Franks, P. J. S. 2002. NPZ models of plankton dynamics: their construction, coupling to physics, and application. J. Oceanogr., *58*(2), 379–387. doi: 10.1023/A:1015874028196

Ganesh, S., L. A. Bristow, M. Larsen, N. Sarode, B. Thamdrup, and F. J. Stewart. 2015. Size-fraction partitioning of community gene transcription and nitrogen metabolism in a marine oxygen minimum zone. ISME J., *9*(12), 2682–2696. doi: 10.1038/ismej.2015.44

Garcia-Robledo, E., S. Borisov, I. Klimant, and N. P. Revsbech. 2016. Determination of respiration rates in water with sub-micromolar oxygen concentrations. Front. Mar. Sci., *3*, 244. doi: 10.3389/fmars.2016.00244

Gong, X. Z., E. Garcia-Robledo, A. Schramm, and N. P. Revsbech. 2016. Respiratory kinetics of marine bacteria exposed to decreasing oxygen concentrations. Appl. Environ. Microbiol., 82(5), 1412–1422. doi: 10.1128/aem.03669-15.

Gutknecht, E., I. Dadou, B. Le Vu, G. Cambon, J. Sudre, V. Garcon, E. Machu, et al. 2013. Coupled physical/biogeochemical modeling including O_2-dependent processes in the Eastern Boundary Upwelling Systems: application in the Benguela. Biogeosciences, *10*(6), 3559–3591. doi: 10.5194/bg-10-3559-2013

Jayakumar, A., B. X. Chang, B. Widner, P. Bernhardt, M. R. Mulholland, and B. B. Ward. 2017. Biological nitrogen fixation in the oxygen-minimum region of the eastern tropical North Pacific ocean. ISME J., *11*(10), 2356–2367. doi: 10.1038/ismej.2017.97

Jensen, M. M., M. M. M. Kuypers, G. Lavik, and B. Thamdrup. 2008. Rates and regulation of anaerobic ammonium oxidation and denitrification in the Black Sea. Limnol. Oceanogr., *53*(1), 23–36. doi: 10.4319/lo.2008.53.1.0023

Jensen, M. M., P. Lam, N. P. Revsbech, B. Nagel, B. Gaye, M. S. M. Jetten, and M. M. M. Kuypers. 2011. Intensive nitrogen loss over the Omani Shelf due to anammox coupled with dissimilatory nitrite reduction to ammonium. ISME J., *5*(10), 1660–1670. doi: 10.1038/ismej.2011.44

Kalvelage, T., M. M. Jensen, S. Contreras, N. P. Revsbech, P. Lam, M. Gunter, J. LaRoche, et al. 2011. Oxygen sensitivity of anammox and coupled N-cycle processes in oxygen minimum zones. PLoS One, *6*(12), e29299. doi: 10.1371/journal.pone.0029299

Kalvelage, T., G. Lavik, M. M. Jensen, N. P. Revsbech, C. Löscher, H. Schunck, D. K. Desai, et al. 2015. Aerobic microbial respiration in oceanic oxygen minimum zones. PLoS One, *10*(7), e0133526. doi: 10.1371/journal.pone.0133526

Keeling, R. F., A. Kortzinger, and N. Gruber. 2010. Ocean deoxygenation in a warming world. Ann. Rev. Mar. Sci., *2*, 199–229. doi: 10.1146/annurev.marine.010908.163855

Keil, R. G., J. N. Neibauer, C. Biladeau, K. van der Elst, and A. H. Devol. 2016. A multiproxy approach to understanding the "enhanced" flux of organic matter through the oxygen deficient waters of the Arabian Sea. Biogeosciences, 13, 2077–2092. doi: 10.5194/bg-13-2077-2016

Lam, P., M. M. Jensen, A. Kock, K. A. Lettmann, Y. Plancherel, G. Lavik, H. W. Bange, and M. M. M. Kuypers. 2011. Origin and fate of the secondary nitrite maximum in the Arabian Sea. Biogeosciences, *8*(6), 1565–1577. doi: 10.5194/bg-8-1565-2011

Lam, P., G. Lavik, M. M. Jensen, J. van de Vossenberg, M. Schmid, D. Woebken, G. Dimitri, et al. 2009. Revising the nitrogen cycle in the Peruvian oxygen minimum zone. Proc. Natl. Acad. Sci. U. S. A., *106*(12), 4752–4757. doi: 10.1073/pnas.0812444106

Loescher, C. R., T. Großkopf, F. D. Desai, D. Gill, H. Schunck, P. L. Croot, C. Schlosser, et al. 2014. Facets of diazotrophy in the oxygen minimum zone waters off Peru. ISME J., *8*(11), 2180–2192. doi: 10.1038/ismej.2014.71

Lutz, M., R. Dunbar, and K. Caldeira. 2002. Regional variability in the vertical flux of particulate organic carbon in the ocean interior. Global Biogeochem. Cycles, *16*(3), 1037. doi: 10.1029/2000gb001383

Morrison, J. M., L. A. Codispoti, S. L. Smith, K. Wishner, C. Flagg, W. D. Gardner, S. Gaurin, et al. 1999. The oxygen minimum zone in the Arabian Sea during 1995. Deep Sea Res. Part II Top. Stud. Oceanogr., 46, 1903–1931. doi: 10.1016/S0967-0645(99)00048-X

Naqvi, W. A. 1991. Geographical extent of denitrification in the Arabian Sea in relation to some physical processes. Oceanol. Acta, *14*(3), 281–290.

Naqvi, S. W. A., M. S. Shailaja, M. Dileep Kumar, and R. Sen Gupta. 1996. Respiration rates in subsurface waters of the northern Indian Ocean: evidence for low decomposition rates of organic matter within the water column in the Bay of Bengal. Deep Sea Res. Part II Top. Stud. Oceanogr., *43*(1), 73–81. doi: 10.1016/0967-0645(95)00080-1

Naqvi, W. S. A., P. V. Narvekar, and E. Desa. 2005. Coastal biogeochemical processes in the North Indian Ocean, *in* The Sea: Ideas and Observations on Progress in the Study of the Seas, A. R. Robinson and K. H. Brink, eds. Volume 14, Part B. Cambridge; Harvard University Press. pp. 723–781.

Penn, J., T. Weber, and C. Deutsch. 2016. Microbial functional diversity alters the structure and sensitivity of oxygen deficient zones. Geophys. Res. Lett., *43*(18), 9773–9780. doi: 10.1002/2016GL070438

Rago, T. A., R. Castro-Valdez, T. Margolina, M. Blum, A. Wheeler, and C. A. Collins. 2013. Physical Measurements of Water Properties Across the Mouth of the Gulf of California during April 2013 (PESCAR24 Cruise)(Mediciones Fisicas de las Propiedades del Agua a Traves de la Boca del Golfo de California Durante Abril de 2013 (Crucero PESCAR24). Monterey: Naval Postgraduate School.

Rao, C. K., S. W. A. Naqvi, M. D. Kumar, S. J. D. Varaprasad, D. A. Jayakumar, M. D. George, and S. Y. S. Singbal. 1994. Hydrochemistry of the Bay of Bengal: possible reasons for a different water-column cycling of carbon and nitrogen from the Arabian Sea. Mar. Chem., *47*(3–4), 279–290. doi: 10.1016/0304-4203(94)90026-4

Revsbech, N. P., L. H. Larsen, J. Gundersen, T. Dalsgaard, O. Ulloa, and B. Thamdrup. 2009. Determination of ultra-low oxygen concentrations in oxygen minimum zones by the STOX sensor. Limnol. Oceanogr. Methods, *7*(5), 371–381. doi: 10.4319/lom.2009.7.371

Rice, C. W., and W. P. Hempfling. 1978. Oxygen-limited continuous culture and respiratory energy conservation in Escherichia coli. J. Bacteriol., *134*(1), 115–124.

Sankar, S., L. Polimene, L. Marin, N. N. Menon, A. Samuelsen, R. Pastres, and S. Ciavatta. 2018. Sensitivity of the simulated Oxygen Minimum Zone to biogeochemical processes at an oligotrophic site in the Arabian Sea. Ecol. Modell. 372, 12–23. doi: 10.1016/j.ecolmodel.2018.01.016

Stolper, D. A., N. P. Revsbech, and D. E. Canfield. 2010. Aerobic growth at nanomolar oxygen concentrations. Proc. Natl. Acad. Sci. U. S. A., *107*(44), 18755–18760. doi: 10.1073/pnas.1013435107

Stramma, L., P. Brandt, J. Schafstall, F. Schott, J. Fischer, and A. Kortzinger. 2008. Oxygen minimum zone in the North Atlantic south and east of the Cape Verde Islands. J. Geophys. Res. Oceans, 113(C4). doi: 10.1029/2007JC004369

Strous, M., J. A. Fuerst, E. H. M. Kramer, S. Logemann, G. Muyzer, K. T. van de Pas-Schoonen, R. Webb, et al. 1999. Missing lithotroph identified as new planctomycete. Nature, *400*(6743), 446–449. doi: 10.1038/22749

Thamdrup, B., T. Dalsgaard, and N. P. Revsbech. 2012. Widespread functional anoxia in the oxygen minimum zone of the Eastern South Pacific. Deep Sea Res. Part I Oceanogr. Res. Pap., *65*, 36–45. doi: 10.1016/j.dsr.2012.03.001

Tiano, L., E. Garcia-Robledo, T. Dalsgaard, A. H. Devol, B. B. Ward, O. Ulloa, D. E. Canfield, and N. P. Revsbech. 2014. Oxygen distribution and aerobic respiration in the north and south eastern tropical Pacific oxygen minimum zones. Deep Sea Res. Part I Oceanogr. Res. Pap., *94*, 173–183. doi: 10.1016/j.dsr.2014.10.001

Tseng, C. P., J. Albrecht, and R. P. Gunsalus. 1996. Effect of microaerophilic growth conditions on expression of the aerobic (cyoABCDE and cydAB) and anaerobic (narGHJI, and dmsABC) respiratory pathway genes in Escherichia coli. J. Bacteriol., *178*(4), 1094–1098.

van de Graaf, A. A., A. Mulder, P. de Bruijn, M. S. M. Jetten, L. A. Robertson, and J. G. Kuenen. 1995. Anaerobic oxidation of ammonia is a biologically mediated process. Appl. Environ. Microbiol., *61*(4), 1246–1251.

Van Mooy, B. A. S., R. G. Keil, and A. H. Devol. 2002. Impact of suboxia on sinking particulate organic carbon: enhanced carbon flux and preferential degradation of amino acids via denitrification. Geochim. Cosmochim. Acta, *66*(3), 457–465. doi: 10.1016/S0016-7037(01)00787-6

Zakem, E. J., and M. J. Follows. 2017. A theoretical basis for a nanomolar critical oxygen concentration. Limnol. Oceanogr., *62*(2), 795–805. doi: 10.1002/lno.10461

Received: *3 December 2018*; revised: *16 September 2019*.